

# Heating Rate Profiles in Galaxy Clusters

Edward C.D. Pope<sup>1,2\*</sup>, Georgi Pavlovski<sup>1</sup>, Christian R. Kaiser<sup>1</sup>, Hans Fangohr<sup>2</sup>

<sup>1</sup>*School of Physics & Astronomy, University of Southampton, UK, SO17 1BJ*

<sup>2</sup>*School of Engineering Sciences, University of Southampton, UK, SO17 1BJ*

10 October 2018

## ABSTRACT

In recent years evidence has accumulated suggesting that the gas in galaxy clusters is heated by non-gravitational processes. Here we calculate the heating rates required to maintain a physically motivated mass flow rate, in a sample of seven galaxy clusters. We employ the spectroscopic mass deposition rates as an observational input along with temperature and density data for each cluster. On energetic grounds we find that thermal conduction could provide the necessary heating for A2199, Perseus, A1795 and A478. However, the suppression factor, of the classical Spitzer value, is a different function of radius for each cluster. Based on the observations of plasma bubbles we also calculate the duty cycles for each AGN, in the absence of thermal conduction, which can provide the required energy input. With the exception of Hydra-A it appears that each of the other AGNs in our sample require duty cycles of roughly  $10^6 - 10^7$  yrs to provide their steady-state heating requirements. If these duty cycles are unrealistic, this may imply that many galaxy clusters must be heated by very powerful Hydra-A type events interspersed between more frequent smaller-scale outbursts. The suppression factors for the thermal conductivity required for combined heating by AGN and thermal conduction are generally acceptable. However, these suppression factors still require ‘fine-tuning’ of the thermal conductivity as a function of radius. As a consequence of this work we present the AGN duty cycle as a cooling flow diagnostic.

**Key words:** hydrodynamics, cooling flows, galaxies: active, galaxies: clusters: individual: (Virgo, A2199, Perseus, Hydra-A, A2597, A1795, A478)

## 1 INTRODUCTION

The radiative cooling times of the hot, X-ray emitting gas in the centres of many galaxy clusters may be as short as  $10^6$  years. In the classical model (see e.g. Fabian 1994, for a review), where radiative losses occur unopposed, a cooling flow develops in which the gas cools below X-ray temperatures and accretes onto the central cluster galaxy where it accumulates in molecular clouds and subsequently forms stars. However, studies have demonstrated both a lack of the expected cold gas at temperatures well below 1-2keV (e.g. Edge 2001) and that spectroscopically determined mass deposition rates are a factor of 5-10 less than the classically determined values (Voigt & Fabian 2004). These findings suggest that the cluster gas is being reheated in order to produce the observed minimum temperatures and the reduction in excess star formation compared to expectations. As yet it is unclear whether this heating occurs continuously or periodically.

There is observational evidence that the temperature profiles of galaxy cluster atmospheres are well described by the same mathematical function across a range in redshift (e.g. Allen et al. 2001). Given such similarity it is possible that the atmospheres of galaxy clusters are in a quasi-steady state and that observable parameters such as the radial temperature profile do not vary significantly over the lifetime of a cluster. This universal temperature profile would be difficult to sustain if the density profiles varied significantly with time. In addition, if large quantities of gas were deposited in the central regions one might expect that the density profiles would be much more centrally peaked than observations suggest. The culmination of this argument is that, at least in the central regions, the inward flow rate of mass must be roughly independent of radius to ensure that mass is not deposited at any particular location which would significantly alter the density profile.

One particular problem with this is that all of the mass flowing in this region must be deposited at the cluster centre. Therefore, unless the mass flow rate is small this would result in large quantities of gas at the cluster centre.

\* E-mail: edpope@soton.ac.uk

In contrast, spectroscopically determined mass deposition rates suggests that mass *is* deposited at a roughly constant rate throughout the cluster, at resolved radii (Voigt & Fabian 2004). However, a roughly constant mass deposition rate is indicative of a mass flow rate that is roughly proportional to radius, rather than constant as the density profiles suggest. Yet, if such a flow were persistent this proportionality would result in density profiles which contradict the observational evidence by being more centrally peaked.

If we are to reconcile the implications of the density profiles and mass deposition rates then one possible explanation is that the mass flow rate exhibits two different asymptotic properties. That is, near the cluster centre or within the central galaxy the mass flow rate should be roughly constant so that the density profiles are essentially left unchanged, while the mass deposited at the cluster centre is sufficiently small to agree with observations. At larger radii the mass flow rate should still be proportional to radius and satisfy the observations on resolvable scales which imply a constant mass deposition rate. The relationship between the mass flow rates and the mass deposition rates are defined section 3.

The two main candidates for heating cluster atmospheres are: Active Galactic Nuclei (AGN) (e.g. Tabor & Binney 1993; Churazov et al. 2001; Brüggén & Kaiser 2002; Brüggén 2003) and thermal conduction (e.g. Gaetz 1989; Zakamska & Narayan 2003; Voigt et al. 2002; Voigt & Fabian 2004). Heating by AGN is thought to occur through the dissipation of the internal energy of plasma bubbles inflated by the AGN at the centre of the cooling flow. Since these bubbles are less dense than the ambient gas, they are buoyant and rise through the intracluster medium (ICM) stirring and exciting sound waves in the surrounding gas (e.g. Ruszkowski & Begelman 2002; Fabian et al. 2002). This energy may be dissipated by means of a turbulent cascade, or viscous processes if they are significant. Deep in the central galaxy other processes such as supernovae and stellar winds will also have some impact on the ambient gas.

However, AGN are only periodically active which could result in similarly periodic heating rates, thus making the possibility of a totally steady state unlikely. In this case one could imagine a scenario in which a quasi steady-state is possible where temperature and density profiles oscillate around their average values. It is also possible that dissipation of the plasma bubbles may occur over timescales longer than the AGN duty cycle thus providing almost continuous heating (e.g. Reynolds et al. 2005).

Thermal conduction may also play a significant role in transferring energy towards central regions of galaxy clusters given the large temperature gradients which are observed in many clusters. In fact, several authors (e.g. Voigt et al. 2002; Voigt & Fabian 2004) have shown that on energy grounds alone it may be possible for thermal conduction to provide the necessary heating in some clusters.

However, the exact value of the thermal conductivity remains uncertain. The theoretical value for the thermal conductivity of a fully ionised, unmagnetised plasma is calculated by Spitzer (1962). Magnetic fields, which are thought to exist in the cluster gas, based on Faraday rotation measures of clusters (e.g. Carilli & Taylor 2002), may greatly alter this value. The standard method by which the unknown

effects of magnetic fields are taken into account is to include a suppression factor,  $f$ , in the Spitzer formula, which indicates the actual value as a fraction of the full Spitzer value.

Several authors have found temperature profiles in some galaxy clusters that are compatible with thermal conduction, and values of the suppression factor that are physically meaningful (e.g. Zakamska & Narayan 2003). In contrast, more detailed work in which the Virgo cluster was simulated using complete hydrodynamics, including radiative cooling and heating by thermal conduction has demonstrated that thermal conduction cannot prevent the occurrence of a cooling catastrophe, in this particular example (Pope et al. 2005). Furthermore, the mass flow rates under such circumstances are not constant with radius so that mass builds up in particular areas and therefore changes the density distribution, making it much more centrally peaked than observed in real clusters.

To answer the questions regarding the necessary heating rates and mechanisms involved in galaxy clusters we construct a simple model based on two main assumptions: galaxy clusters are in approximate steady state, and the mass flow rates fulfill the constraints provided by observations at both large and small radii. To ensure this, the radial behaviour of the mass flow rates is modelled using an observationally motivated, but empirical function consistent with the observations. Using mathematical functions fitted to the temperature and density data of seven galaxy clusters we derive the required heating rates within regions which are consistent with those for which the mass flow rates were determined. We also compare the observed energy currently available in the form of plasma bubbles with the heating requirements for each cluster. From the heating rate profiles we calculate the thermal conduction suppression factor as a radial function for each cluster in order that we may determine which clusters could be heated by this process.

The plan for this paper is as follows. In Section 2 we give the details of the parameters used to fit observational temperature and density data for seven galaxy clusters. In Section 3 and 4 we describe the model used to estimate the required heating, and thermal conduction suppression factors. The heating rates we have calculated are compared with observational estimates of both AGN heating and a combination of AGN heating and thermal conduction in Sections 5 and 6. In Section 7 we summarize our main findings.

The results are given for a cosmology with  $H_0 = 70\text{kms}^{-1}\text{Mpc}^{-1}$ ,  $\Omega_M = 0.3$  and  $\Omega_\Lambda = 0.7$ .

## 2 FUNCTIONS FITTED TO OBSERVATIONAL DATA

In this section we give details of the functions used to derive the mass deposition and heating rate profiles, the references to the observational data, and show a comparison with the data in figure 1.

We have only fitted our own functions to the data when the original authors had not included confidence intervals for their model parameters, but we give the functions used to fit all of the cluster atmospheres. The values of the fitted parameters are given in tables 1 and 2.

Name	$n_0(\text{cm}^{-3})$	$n_1(\text{cm}^{-3})$	$\beta_0$	$\beta_1$	$r_0(\text{kpc})$	$r_1(\text{kpc})$
Virgo	$0.089 \pm 0.011$	$0.019 \pm 0.002$	$1.52 \pm 0.32$	0.705	$5 \pm 1$	$23.3 \pm 4.3$
Perseus	$0.071 \pm 0.003$		$0.81 \pm 0.04$		$28.5 \pm 2.7$	
Hydra	$0.07 \pm 0.02$		$0.72 \pm 0.004$		$18.6 \pm 0.5$	
A2597	$0.13 \pm 0.07$		$0.15 \pm 0.10$	$0.79 \pm 0.06$	$1.0 \pm 2.6$	$43 \pm 14$
A2199	0.19		0.75		1	
A1795	$0.066 \pm 0.067$		$0.24 \pm 0.11$	$0.41 \pm 0.13$	$57 \pm 37$	$12 \pm 4.9$
A478	$0.153 \pm 0.019$		$0.55 \pm 0.05$	$0.41 \pm 0.34$	$145 \pm 32$	$6.6 \pm 1.9$

**Table 1.** Summary of best fit parameters for density profiles with 1-sigma errors obtained from the least-squares fitting procedure. We do not give errors the model function parameters for A2199 since we were unable to obtain the observational data. See table 2 for references.

The Virgo cluster's electron number density data was fitted by Ghizzardi et al. (2004) using a double  $\beta$ -profile,

$$n = \frac{n_0}{[1 + (r/r_0)^2]^{\beta_0}} + \frac{n_1}{[1 + (r/r_1)^2]^{\beta_1}}. \quad (1)$$

For simplicity, the Perseus (see Sanders et al. 2004) and Hydra (David et al. 2001) density data were fitted with single  $\beta$ -profiles,

$$n = \frac{n_0}{[1 + (r/r_0)^2]^{\beta_0}}. \quad (2)$$

We were unable to obtain the observational data for A2199 and so relied on the fits presented by the original authors (Johnstone et al. 2002) who found that a simple power-law was sufficient to describe the density distribution,

$$n = n_0 \left( \frac{r}{r_0} \right)^{-\beta_0}. \quad (3)$$

For A2597, A1795 and A478 (see McNamara et al. 2001; Ettori et al. 2002; Sun et al. 2003, respectively) we employ the function used by Dennis & Chandran (2005) to fit the density distributions,

$$n = \frac{n_0}{[1 + (r/r_0)^2]^{\beta_0}} \frac{1}{[1 + (r/r_1)^2]^{\beta_1}}. \quad (4)$$

As above, for the cluster gas temperature profiles we have only fitted functions to the data when the original authors had not included confidence intervals, but give the details for all clusters in our sample.

Ghizzardi et al. (2004) found that the Virgo temperature data is best described by a Gaussian curve,

$$T = T_0 - T_1 \exp\left(-\frac{1}{2} \frac{r^2}{r_{\text{ct}}^2}\right). \quad (5)$$

Churazov et al. (2003) fitted the Perseus temperature data with the function,

$$T = T_0 \left[ \frac{1 + (r/r_{\text{ct}})^3}{\delta + (r/r_{\text{ct}})^3} \right]. \quad (6)$$

We fitted the temperature data for A2597, A1795 and A478 using the same function as Dennis & Chandran (2005),

$$T = T_0 - \frac{T_1}{[1 + (r/r_{\text{ct}})^2]^{\delta}}. \quad (7)$$

The best-fit temperature profile for the Hydra cluster is given by David et al. (2001) as a power-law,

$$T = T_0 \left( \frac{r}{r_{\text{ct}}} \right)^{\delta}. \quad (8)$$

The A2199 temperature data was found by the original authors (Johnstone et al. 2002) to be described by a power-law without a characteristic length-scale. For consistency we use equation (8) to represent the temperature distribution in this cluster.

Although we have provided 1-sigma errors for the fitted parameters that describe the temperature and density distribution of the gas in galaxy clusters, we will not give errors for any quantities derived from these parameters. The reason for this is that the errors and gradients of the temperature and density are all model dependent. In addition, the calculations are complex, making the standard propagation of errors impractical and error estimates themselves very uncertain. In addition, although we can make very conservative estimates of the confidence limits, of a particular derived quantity, they are too vague to be of importance.

### 3 THE MODEL

#### 3.1 General heating rates

Starting from the assumption that the atmospheres of galaxy clusters are spherically symmetric, and in a quasi steady-state, it is possible to derive what the time averaged heating rate, as a function of radius, must be in order to maintain the observed temperature and density profiles,

$$h = n^2 \Lambda_{\text{rad}} + \frac{1}{r^2} \frac{d}{dr} \left[ \frac{\dot{M}}{4\pi} \left( \frac{5k_{\text{b}}T}{2\mu m_{\text{p}}} + \phi \right) \right], \quad (9)$$

Name	$T_0$ (keV)	$T_1$ (keV)	$r_{ct}$ (kpc)	$\delta$	Reference
Virgo	2.4±0.1	0.77±0.10	23±4		1
Perseus	8.7±1.1		63±5	2.7±0.3	2
Hydra	2.73±0.07		10	0.12±0.01	3
A2597	4.1±0.1	2.0±0.2	16±10	0.7±0.4	4,5
A2199	1.0		1	0.29	6
A1795	7.2±1.9	5.1±2.2	40±34	0.5±0.7	7,5
A478	9.7±1.5	7.6±1.7	16±5	0.3±0.2	8,5

**Table 2.** Summary of temperature parameters fitted to the data with 1-sigma errors obtained from the least-squares fitting procedure. References:-(1) Ghizzardi et al. (2004); (2) Sanders et al. (2004); (3) David et al. (2001); (4) McNamara et al. (2001) and Rafferty et al. (2005), in preparation; (5) Dennis & Chandran (2005); (6) Johnstone et al. (2002); (7) Ettori et al. (2002); (8) Sun et al. (2003). We do not give errors for A2199 since we were unable to obtain the observational data. We also do not give an error for the Hydra temperature scale-height since none was given in the original publication, David et al. (2001).

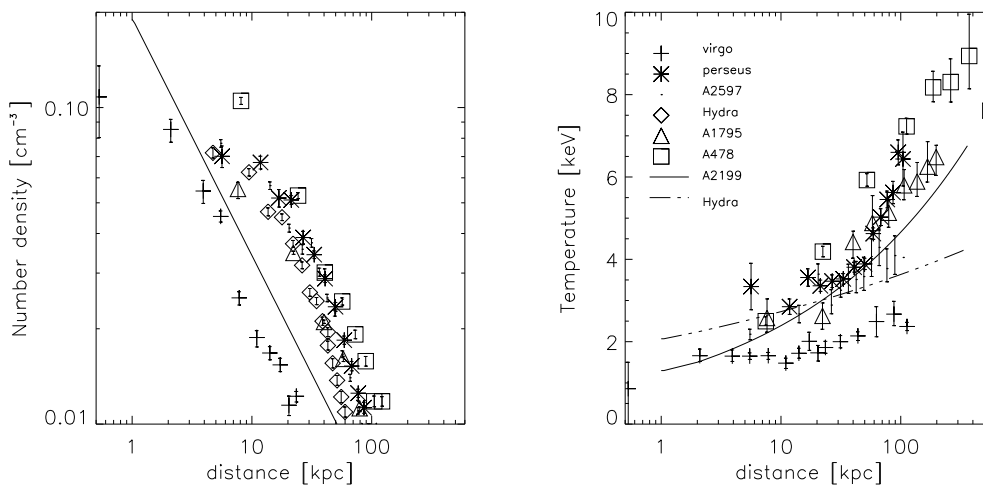


**Figure 1.** Left: density data for all clusters except A2199 for which we show the best-fit, since we did not have access to the observational data. Right: temperature data except for A2199 and Hydra for which we give the fitted functions, since we did not have access to the observational data. The key in the right-hand panel applies to both temperature and density data.

where  $\dot{M}$  is the mass flow rate,  $T$  is the gas temperature,  $n$  is the gas number density,  $\Lambda_{\text{rad}}$  is the cooling function and  $\phi$  is the gravitational potential. Here we assume only subsonic flow of gas.

The mass flow rate through a spherical surface, radius  $r$ , is

$$\dot{M} = 4\pi r^2 \rho v_r, \quad (10)$$

where  $\rho$  is the gas density and  $v_r$  is the gas velocity in the radial direction.

The difference between the rate at which mass enters and leaves a spherical shell, of thickness  $\Delta r$ , is called the mass deposition rate,  $\Delta \dot{M}$ . In terms of the mass flow rate, the mass deposition rate is

$$\Delta \dot{M} \approx \left( \frac{d\dot{M}}{dr} \right) \Delta r \quad (11)$$

Consequently, the mass flow rate, at a particular radius, can be recovered by summing the contributions of the mass deposition rate in each shell up to that radius. Henceforth, we refer to the mass flow rate as the integrated mass deposition rate.

For subsonic gas flow the cluster atmosphere can be assumed to be in approximate hydrostatic equilibrium. On this basis, we are able to estimate the gravitational acceleration from the temperature and density profiles of the cluster atmosphere,

$$\frac{dP}{dr} = -\rho \frac{d\phi}{dr}, \quad (12)$$

where  $P$  is the gas pressure and  $\rho$  is the gas density.

The gas pressure is related to density and temperature by the ideal gas equation

$$P = \frac{\rho k_b T}{\mu m_p}, \quad (13)$$

where  $\mu m_p$  is the mean mass per particle. We assume that  $\mu=16/27$  as appropriate for standard primordial abundance.

To avoid anomalies when calculating spatial derivatives, we fit continuous analytical functions through the density and temperature data in the previous section. This ensures that we do not encounter any large discontinuities which may result in extreme heating rates.

The only unknowns in equation (9) are then the integrated mass deposition rate,  $\dot{M}$ , and the heating rate,  $h$ .

### 3.2 Calculating Mass Deposition rates

In the classical cooling flow picture, which assumes that the heating is zero everywhere, and ignoring the effect of the gravitational potential, the bolometric X-ray luminosity, integrated mass deposition rate and gas temperature are related by integrating equation (9) (e.g. Fabian 1994) over a spherical volume. Analytically, the bolometric X-ray luminosity within a given radius is simply the volume integral of the radiative cooling rate per unit volume,

$$L_X(< r) = 4\pi \int_0^r n^2 \Lambda_{\text{rad}} r^2 dr. \quad (14)$$

Integrating the second term in equation (9) gives the relationship between bolometric luminosity, integrated classical mass deposition rate and temperature,

$$L_X(< r) = \frac{5k_b}{2\mu m_p} \dot{M}_{\text{clas}}(r) T(r). \quad (15)$$

For observational data the luminosity and classical mass deposition rates at each radius are estimated by dividing the observed 2-d projection of the cluster into concentric shells. Using this method one is able to reconstruct the 3-d properties of a cluster. The contribution, to the total X-ray luminosity, of the  $j$ th spherical shell, of thickness  $\Delta r$ , is then calculated by discretizing equation (15),

$$\Delta L_{Xj} = \frac{5k_b}{2\mu m_p} (\dot{M}_{\text{clas}j} \Delta T_j + \Delta \dot{M}_{\text{clas}j} T_j). \quad (16)$$

In any given shell, the term involving  $\Delta T_j$  is assumed to be small compared to the term involving  $\Delta \dot{M}_{\text{clas}j}$ . By ignoring the  $\Delta T_j$  term the resulting mass deposition rate is larger than it would be if the change in temperature across the shell was taken into account. Therefore, the classical value is the absolute maximum possible mass deposition rate. The luminosity of a given shell is then assumed to be (e.g. Voigt & Fabian 2004),

$$\Delta L_{Xj} = 4\pi r^2 \Delta r n^2 \Lambda_{\text{rad}} = \frac{5k_b T_j}{2\mu m_p} \Delta \dot{M}_{\text{clas}j}. \quad (17)$$

Therefore, the rate at which mass is deposited within the  $j$ th shell is

$$\Delta \dot{M}_{\text{clas},j} = \frac{4\pi r_j^2 \Delta r n_j^2 \Lambda_{\text{rad}}}{\frac{5k_b T_j}{2\mu m_p}}. \quad (18)$$

The total X-ray luminosity emitted by the gas within a particular radius is calculated by summing the contributions from all of the shells within this radius

$$L_X(< r) = \frac{5k_b}{2\mu m_p} \dot{M}_{\text{clas}}(< r) T(r), \quad (19)$$

where  $\dot{M}_{\text{clas}}(< r)$  is the integrated mass deposition rate obtained by summing the contribution from each shell within the radius,  $r$ .

If we include a heating term the expression equivalent to equation (15) becomes,

$$L_X(< r) - H(< r) = \frac{5k_b}{2\mu m_p} \dot{M}_{\text{cool}} T(r), \quad (20)$$

where  $\dot{M}_{\text{cool}}$  is the integrated mass deposition rate, resulting from the excess of cooling over heating. This integrated mass deposition rate is distinct from the integrated classical mass deposition rate which is only used to describe the situation in the absence of heating.

With equation (16) becomes,

$$\Delta(L_{X,j} - H_j) = \frac{5k_b}{2\mu m_p} (\dot{M}_{\text{cool},j} \Delta T_j + \Delta \dot{M}_{\text{cool},j} T_j). \quad (21)$$

In practice, a realistic estimate of the mass deposited into each shell, which takes into account heating, can be obtained by fitting models to the X-ray spectrum of each shell or a larger region if desired. The spectroscopic mass deposition rate is just a fitting parameter in this case and an integrated value can be obtained in exactly the same way as for the classical case above.

Generalising equation(19) to allow for heating we find that if the spectroscopically determined mass deposition rate,  $\dot{M}_{\text{obs}}$ , is representative of the actual mass deposition rate,  $\dot{M}_{\text{cool}}$ , then one can determine the heating rate from,

$$L_X(< r) - H(< r) = \frac{5k_b}{2\mu m_p} \dot{M}_{\text{obs}}(< r) T(r) = \frac{5k_b}{2\mu m_p} \dot{M}_{\text{cool}} T(r). \quad (22)$$

If the spectroscopically determined value for the mass deposition rate is a true representative of the real mass deposition rate, then the integral within the cooling radius is simply the integrated mass deposition rate within the cooling radius, irrespective of the radial distribution. Therefore, it would seem a sensible starting point for any calculations of the heating rates in galaxy clusters. To ensure consistency between theory and observations, we must employ the same mass flow rate (integrated mass deposition rate) over the same region, in our heating models. Consequently, if we use the observed spectroscopic mass deposition rate integrated up to the cooling radius, then to be strictly accurate, the heating rates we subsequently calculate are only valid up to this radius.

### 3.3 Model Integrated Mass Deposition Rates

We now construct a model for the integrated mass deposition rate in galaxy clusters on the basis of the observational evidence. Although the model function is essentially empirical there are three main constraints to which it must adhere. These are: firstly, the fact that the observed spectroscopic mass deposition rate in each shell is approximately constant up to the cooling radius suggests linear dependence of flow rate on radius. Secondly, the observed density profiles also suggest that the mass deposition rate is negligible near the cluster centre. Otherwise a pronounced peak would be observed in the density profiles. Thirdly, the integrated mass deposition rate at the cooling radius must be equal to the observed integrated mass deposition rate at that location. A simple empirical form for the integrated mass deposition rate which is, in some way, consistent with the above is

$$\dot{M}(r) = \dot{M}_{\text{obs}}(< r_{\text{cool}}) \left[ K + \left( \frac{r}{r_{\text{cool}}} \right)^2 \right]^{0.5}, \quad (23)$$

where  $\dot{M}_{\text{obs}}(< r_{\text{cool}})$  is the integrated spectroscopic mass deposition rate at the cooling radius,  $K$  is a constant and  $r_{\text{cool}}$  is the cooling radius.

To estimate  $K$  we express it the following way,  $K = (r_{\text{K}}/r_{\text{cool}})^2$ , where  $r_{\text{K}}$  is a length scale corresponding to  $K$ . A suitable value for  $r_{\text{K}}$  is the radius of the central galaxy, roughly 30 kpc, since the effect of the interstellar medium is likely to significantly alter the inflow of material. This leads to values for  $K$  ranging from 0.73, for Virgo, to 0.04, for A478.

Note that our expression for  $\dot{M}$  implies that  $d\dot{M}/dr = 0$  for small radii, meaning that no material is deposited. However, at or near  $r = 0$  the material must be deposited since it cannot flow to negative radii. This can account for the excess star formation which is observed to occur in these regions. For reasonable gradients of the temperature distribution, the second term on the right hand side of equation (9) then tends to infinity as  $r$  tends to zero. This implies that our model predicts negative heating rates,  $h$ , for small radii. In other words, the model is only valid outside the region at the very centres of clusters. To indicate the range over which our model can provide physically meaningful predictions, we list in Table 3, the minimum radius for each cluster at which  $h=0$ . We take this minimum radius as the lower integration limit in our calculation of the total heating rates.

For each cluster the observations are inevitably limited by spatial resolution and in some cases the lower integration limits, explained above, occur at radii which are closer to the cluster centre than the spatial resolution limits. In principle, the spatial resolution presents a limit beyond which we are unable to accurately describe the temperature and density of the cluster gas. However, because we have fitted analytical functions to the temperature and density data for each cluster we can extrapolate the behaviour of the temperature and density, and hence the heating rates, from the data point nearest the cluster centre further towards the centre. The results at  $r < r_{\text{min}}$  should be ignored as we have no observational information to constrain them.

### 3.4 Thermal conduction

Thermal conduction of heat from the cluster outskirts to their centres may provide the required heating of the central regions without an additional energy source, like an AGN (e.g. Gaetz 1989; Zakamska & Narayan 2003; Voigt & Fabian 2004). Of course, thermal conduction only transports energy from one region to another and does not lead to net heating. However, if we consider the case for which there is an infinite heat bath at large radii, then any drop in temperature at large radii, due to the inward transfer of thermal energy, is negligible.

Several 1-d models have been able to achieve a steady-state using thermal conduction alone (e.g. Zakamska & Narayan 2003) and the combined effects of thermal conduction and AGNs (e.g. Brüggen 2003; Ruszkowski & Begelman 2002). We, therefore, compare the required heating rates with an estimate of the energy transport supplied by thermal conduction given the current state of each galaxy cluster.

The volume heating rate for thermal conduction from an infinite heat bath is given by

$$\epsilon_{\text{cond}} = \frac{1}{r^2} \frac{d}{dr} \left( r^2 \kappa \frac{dT}{dr} \right), \quad (24)$$

where  $\kappa$  is the thermal conductivity and  $dT/dr$  is the temperature gradient.

We take the thermal conductivity to be given by Spitzer (1962), but include a suppression factor,  $f(r)$ , defined in the introduction, to take into account the effect of magnetic fields,

$$\kappa = \frac{1.84 \times 10^{-5} f(r) T^{5/2}}{\ln \Lambda_c}, \quad (25)$$

where  $\ln \Lambda_c$  is the Coulomb logarithm.

For pure hydrogen the Coulomb logarithm is (e.g. Choudhuri 1998)

$$\Lambda_c = 24\pi n_e \left( \frac{8\pi e^2 n_e}{k_b T} \right)^{-3/2}, \quad (26)$$

where  $n_e$  is the electron number density.

For a steady-state to exist, the heating by thermal conduction must be equal to the heating rate,

$$\epsilon_{\text{cond}} = -h, \quad (27)$$

where  $h$  is the required heating rate per unit volume, given by equation (9).

This is essentially the same energy equation as solved by (e.g. Zakamska & Narayan 2003), although we also allow for mass deposition, line-cooling and variations in the Coulomb logarithm. We then solve equation (27), using the observed temperature and density profiles, to determine the radial dependence of the suppression factor. This is different to the approach of (Zakamska & Narayan 2003). In their paper they use the same equations to calculate temperature and density profiles that are consistent with a constant suppression factor. These derived profiles are only constrained by observations at the minimum and maximum radii acces-

sible to observations. We take the density and temperature profiles from the observed data and allow the suppression factor to vary with radius.

Our function for the suppression factor is obtained by integrating both sides of equation (27) over a spherical surface and then rearranging for  $f$ ,

$$f(r) = \frac{\int_{r_{\min}}^r r^2 h(r) dr}{1.84 \times 10^{-5} r^2 dT/dr T^{5/2} / \ln \Lambda_c}. \quad (28)$$

We note that the energy flux due to thermal conduction,  $\kappa dT/dr$ , increases with radius so that, for an infinite heat bath at large radii, energy must always be deposited at each smaller radius, rather than taken away.

## 4 RESULTS:1

### 4.1 Comparison of Luminosities

To ensure that our estimates are compatible with those calculated from observations we compare the bolometric X-ray luminosities, within the cooling radius, determined from our functions fitted to the data and the observed luminosities presented in Birzan et al. (2004). We assume half solar metallicity for all clusters and use the cooling function as given in Sutherland & Dopita (1993).

Table 3 demonstrates reasonable agreement between the results obtained using the fitted functions and those presented in Birzan et al. (2004).

### 4.2 Integrated Mass Deposition rates

Since the values of the integrated mass deposition rates that we use are critical to determining the heating rates, we present these first. In table 4 we compare the integrated spectroscopic mass deposition rate,  $\dot{M}_{\text{spec}}(< r_{\text{cool}})$  (Birzan et al. 2004), with the integrated classical mass deposition rate,  $\dot{M}_{\text{clas}}(< r_{\text{cool}})$  (Fabian 1994) at the cooling radius, and the central integrated mass deposition rate predicted by equation (23).

From equation (20) it is clear that the spectroscopic mass deposition rates are indicative of the energy injected into the cluster. Because of this, the spectroscopic mass deposition rate should be less than the classical value, depending upon the relative magnitudes of the heating and cooling, as is the case. However, because of the time taken to dissipate this injected energy into the ambient gas this implies that the current spectroscopic mass deposition rates are a function of the heating which has taken place over the last few times  $10^8$  yrs.

The central integrated mass deposition rates predicted by equation (23) are sufficiently low that the total mass deposited in the cluster centre, over a Gyr, will not significantly alter the total central mass. It should be noted that a smaller value of the constant,  $K$ , in equation (23), would result in still smaller central integrated mass deposition rates.

### 4.3 Required Heating rates and Thermal Conduction Suppression factors

The heating rates are shown in figure 2, for the form of integrated mass deposition rates given in equation (23). For comparison, we also show the volume heating rate profiles for unsuppressed thermal conduction.

Figure 2 shows that the heating rates for the entire sample of clusters exhibit similar profiles. This is because the radiative losses most strongly depend upon the density, therefore so must the required heating rate. Since the majority of the density profiles are described by  $\beta$ -profiles, this similarity is expected.

In comparison, it is clear that the volume heating rates for unsuppressed thermal conduction vary from cluster to cluster and do not share the same profile as the required heating rates. Even for the clusters in which thermal conduction can supply the necessary energy, the different radial dependences require that the suppression factor is fine-tuned to provide the correct heating rate for all radii. This demonstrates the different nature of the physical processes involved in radiative cooling and thermal conduction, making a balance between the two hard to achieve.

Using equation (28) we calculate the thermal conduction suppression factor, as a function of radius, for which the required heating rate is achieved. These results, plotted in figure 3, suggest that thermal conduction could provide the required heating rates in A2199, A478, Perseus and very nearly A1795. It seems impossible that thermal conduction would be able to transport sufficient energy towards the central regions for the remainder of the sample.

It is evident that the suppression factor profiles are different in almost every case, although A1795 and A478 appear to have certain features in common. The only common trait is that the required suppression factor tends to be largest near the centre, except for A2597 and Hydra. This suggests that even in the regions where the suppression factor takes physically meaningful values ( $f < 1$ ), in order for thermal conduction to provide the necessary heating, the parameters which determine the suppression factor require unique fine tuning in each cluster. We note that suppression factors of greater than unity are unphysical for laminar flows but are possible in mixing layers (e.g. Cho et al. 2003).

Our suppression factors can be compared with those found by Zakamska & Narayan (2003) who studied four of the clusters in our sample. They find suppression factors of 1.5, 2.4, 0.4 and 0.2 for Hydra, A2597, A2199 and A1795 respectively. These values agree with our results in that we also find that thermal conduction must take unphysically large values for Hydra and A2597 and realistic values for the remaining two clusters. Voigt & Fabian (2004) also provide a suppression factor, roughly 0.2-0.3, for A478 which is consistent with, albeit lower than, the possible values we have found for the same cluster.

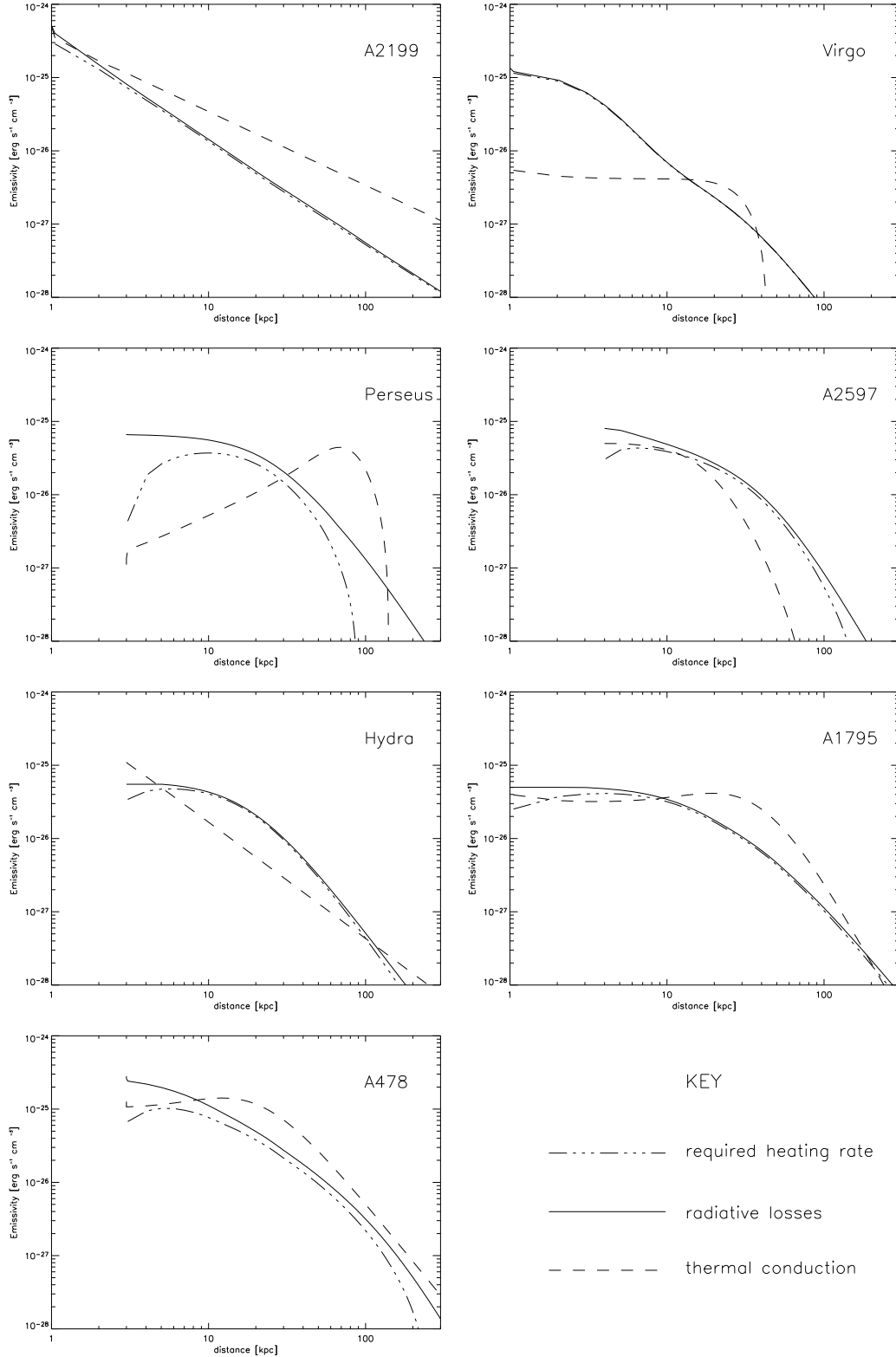


**Figure 2.** Comparison of cooling and heating rate profiles for each cluster. The heating rates fall to zero at a radius which depends upon the mass deposition rate. At the point at which this occurs, we also terminate each of the other curves since we cannot determine the gas properties within this radius.

Name	$L_X(r_{\text{cool}})/10^{42}\text{ergs}^{-1}$	$L_X(r_{\text{cool}})/10^{42}\text{ergs}^{-1}$	$r_{\text{cool}}/kpc$	$r_{\text{min}}/kpc$
Virgo	10.7	$9.8^{+0.8}_{-0.7}$	35	1
Perseus	550	$670^{+40}_{-30}$	102	3
Hydra	243	$250^{+15}_{-15}$	100	3
A2597	470	$430^{+40}_{-30}$	129	4
A2199	156	$150^{+10}_{-10}$	113	1
A1795	493	$490^{+30}_{-30}$	137	1
A478	1494	$1220^{+60}_{-60}$	150	3

**Table 3.** Comparison of bolometric luminosities derived from our functions fitted to the data (column 2) with those given in Birzan et al. (2004) (column 3), the cooling radius (column 4) and the lower integration limits (column 5).

Name	$\dot{M}_{\text{spec}}(< r_{\text{cool}})$	$\dot{M}_{\text{clas}}(< r_{\text{cool}})$	$\dot{M}_{\text{spec}}(< r_{\text{cool}})\frac{r_K}{r_{\text{cool}}}$
Virgo	$1.8^{+1.2}_{-0.16}$	10	1.3
Perseus	$54^{+48}_{-18}$	183	4.7
Hydra	$14^{+9}_{-7}$	315	1.3
A2597	$59^{+40}_{-40}$	480	3.2
A2199	$2^{+7}_{-1.9}$	150	0.1
A1795	$18^{+12}_{-10}$	478	0.9
A478	$150^{+60}_{-68}$	570	6

**Table 4.** Mass deposition rate parameters (all quantities in solar masses per year). The integrated spectral mass deposition rates are taken from Birzan et al. (2004) and the classically determined values are from Fabian (1994) and references therein. The central mass flow rates calculated using equation (23) are also shown for comparison.

## 5 COMPARISON OF REQUIRED HEATING RATES WITH OBSERVATIONS

### 5.1 Comparison with AGN

The time-averaged mechanical luminosity of a central AGN in each cluster is estimated using

$$\langle L_{\text{mech}} \rangle = \frac{\alpha PV}{t}, \quad (29)$$

where  $\alpha=16$ .  $P$  is the ambient cluster gas pressure,  $V$  is the bubble volume and  $t$  is the estimated duty cycle for an AGN. We assume initially that the duty cycle of each AGN is  $10^8$  yrs. The factor 16 arises from 2 bubbles per outburst, a factor of 2 for the energy dissipated in the shock expansion of the bubble and 4 for  $\gamma/(\gamma-1)$  where  $\gamma = 4/3$  for relativistic gas.

This is simply an estimate of the rate at which energy is injected into the cluster, by the central AGN, and is not related to any particular physical process by which this energy is dissipated e.g. the viscous dissipation of sound waves or effervescent heating.

The estimated AGN power injection rates are given in column 2 of Table 5. To compare the required heating rates with the observational estimates of AGN heating in equation (29) we must calculate the volume integral of equation (9). From this we can estimate the heating luminosity required within a given volume to satisfy the requirements of the assumed steady-state. Comparing this value with that of the power output from AGNs at the centres of galaxy clusters allows us to estimate the frequency with which buoyant plasma bubbles, identical to those currently observed, must be produced in order to provide sufficient heating within the cooling radius. This is defined as the AGN duty cycle, which may be calculated using

$$\frac{4\pi \int_{r_{\text{min}}}^{r_{\text{cool}}} r^2 h dr}{\langle L_{\text{mech}} \rangle} = \frac{t}{\tau}, \quad (30)$$

where  $r_{\text{cool}}$ , the upper integration limit, is the cooling radius and  $r_{\text{min}}$  is the radius at which the heating rate tends to zero for our chosen descriptions of the mass flow rate,  $\tau$  is the calculated duty cycle and  $t$  is the time defined in equation (29).

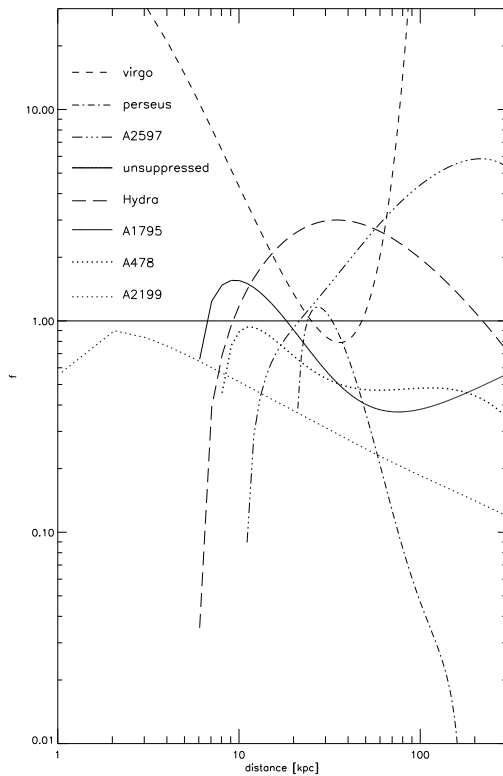


**Figure 3.** Thermal conduction suppression factors for the sample of seven clusters. The thick, solid line shows the maximum physically meaningful suppression factor ( $f=1$ ) for comparison.

## 5.2 The Combined Heating by Thermal Conduction and AGN

To estimate the total rate of energy injection by AGNs into the cluster gas within the cooling radius we assume that all of the energy available in the bubbles is dissipated within the cooling radius. Furthermore, the integral of equation (24) over a spherical surface gives the rate at which thermal conduction transfers heat across a radius,  $r$ ,

$$L_{\text{cond}}(r) = 4\pi r^2 \kappa \frac{dT}{dr}. \quad (31)$$

The maximum total rate at which energy can be injected into this region is the sum of these two processes. We compare this sum with the heating rate required for steady-state and allowing for mass deposition. Within the cooling radius, we can then determine the thermal conduction suppression factor required to maintain a steady-state given the current AGN heating rate. This suppression factor is calculated using

$$f = \frac{L_{\text{heat}}(< r) - \langle L_{\text{mech}} \rangle}{L_{\text{cond}}(r)}, \quad (32)$$

where  $L_{\text{heat}}(< r)$  is the required heating rate for the spherical volume within  $r$ ,  $\langle L_{\text{mech}} \rangle$  is the current mechanical power of the AGN assuming a duty cycle of  $10^8$  yrs.

## 6 RESULTS:2

### 6.1 AGN Duty Cycles

The duty cycles (see Table 5) for Virgo and A478 are of the order of  $10^6$  yrs which is very short compared to the predicted lifetimes of AGN (e.g. Nipoti & Binney 2005, and references therein). In contrast, the Hydra cluster requires recurrent outbursts of magnitude similar to the currently observed one only every  $10^8$  yrs, or so. The required duty cycles for the remaining AGNs are of the order of  $10^7$  yrs. From this we conclude that if thermal conduction is negligible and if this sample is representative of galaxy clusters in general, then many if not all clusters will probably be heated, at certain points in time, by extremely powerful AGN outbursts. However, it is worthwhile pointing out that roughly 71% of cD galaxies at the centres of clusters are radio-loud (Burns 1990) which is larger than for galaxies not at the centres of clusters. This may suggest that the galaxies at the centres of clusters are indeed active more frequently than other galaxies. It is possible that a combination of these two effects satisfies the heating requirements we have identified.

In contrast to the spectroscopically derived mass deposition rates, the plasma bubbles, that still exhibit radio emission and are currently observable, are probably more indicative of the current heating rate rather than the heating rate over the previous  $10^9$  years, or so. If this is true, only Hydra is currently being excessively heated in our small sample.

Our results also show that the gas outside the cooling radius requires significant amounts of energy to allow a

steady-state. Given the large heating requirements for the regions outside the cooling radii of Virgo, A2199 and A478, it is reasonable to ask whether it is possible for the observed plasma bubbles in these clusters to deliver energy at such large radii. The observational evidence (e.g. Birzan et al. 2004) seems to show that bubbles rarely rise to beyond 40 kpc from the cluster centre and in general tend to reach only a few tens of kiloparsecs. This may be because beyond these radii, hydrodynamic instabilities have shredded the bubbles (e.g. Kaiser et al. 2005; Reynolds et al. 2005; Robinson et al. 2004; Churazov et al. 2001), or alternatively the isentropy radius at which the bubbles spread out and form pancakes is generally at radii of these magnitudes (e.g. Churazov et al. 2001). Alternatively, the apparent absence of bubbles at larger radii may be a selection effect since they are harder to detect against the rapidly declining X-ray surface brightness profiles. In any case, it is possible that extremely powerful outbursts with highly extended jets such as Hydra-A or Cygnus-A type events are the best mechanism by which energy is supplied to such large radii, since they cannot be reached by smaller scale outbursts.

## 6.2 The Combined Heating by Thermal Conduction and AGNs

From table 5 it is clear that A2597 is currently being heated insufficiently by the combined effects of AGN and thermal conduction. Thus, it seems that the only way that A2597 can avoid a cooling catastrophe is by an exceptionally large AGN outburst which will have to be roughly 100 times more powerful than the current outburst in order to provide sufficient heating. Of the other clusters in this sample, the suppression factors are all physically acceptable except for Hydra. The reason for this and the negative value of the suppression factor for Hydra is that the energy of the current AGN outburst exceeds the heating requirements within the cooling radius. However, the errors associated are relatively large so it is difficult to say with any certainty if a combination of heating by thermal conduction and AGN can achieve a steady-state.

Although the global suppression factor for thermal conduction is physically acceptable, it still requires fine-tuning inside each cluster to allow a steady-state (see Section 4.3).

## 7 SUMMARY

In the heating of intracluster gas, the energy input required from AGNs is likely to depend on the strength of any other heating processes. For example, if thermal conduction is present and can reduce the integrated mass deposition rate towards the cluster centre, it is likely that in this case the AGN outbursts will have to be less powerful than in an otherwise identical cluster in which thermal conduction does not occur. There may also be additional heating processes such as stirring by galaxy motions or the gas motion resulting from past cluster-cluster mergers.

We have calculated the heating rates required to maintain a steady state for a sample of seven galaxy clusters with the assumption that the mass flow rates are independent of radius. For our model we use the spectroscopically determined integrated mass deposition rates. Here we summarise

our main findings for each cluster in our sample in terms of the mass deposition rates, thermal conduction and required AGN duty cycles.

A2199: It appears that, without AGN heating, thermal conduction is sufficient for the steady-state heating requirements. In the absence of thermal conduction, the required AGN duty cycle of roughly  $10^7$  yrs is short, but still compatible with predicted AGN lifetimes. When we consider simultaneous heating by both AGN, based on the current outburst, and thermal conduction, the suppression factor necessary to satisfy the heating requirements within the cooling radius is roughly 0.16 which is acceptable.

Virgo: Even allowing for mass deposition, thermal conduction alone is insufficient for providing the heating requirements at all radii. The required AGN duty cycle, in the absence of thermal conduction, of roughly  $10^6$  yrs is very short compared with predicted AGN lifetimes suggesting that significantly larger AGN outflows are required at certain intervals to prevent a cooling catastrophe. This is interesting since Virgo has the smallest heating requirement in our sample. Within the cooling radius, the combined effect of the current AGN outburst and thermal conduction can achieve the required heating with a suppression factor of 0.7.

Perseus: It seems that in the absence of an AGN, thermal conduction may be insufficient compared to heating requirements at roughly roughly the central 30 kpc, but may be sufficient outside this radius. Without thermal conduction, the required AGN duty cycle of roughly  $3 \times 10^7$  yrs is also compatible with predicted AGN lifetimes. The suppression factor for the combined effect of AGN and thermal conduction to provide the required heating is 0.05.

Hydra: Thermal conduction alone cannot provide the necessary heating for maintaining a steady-state. The required AGN duty cycle in the absence of thermal conduction is long compared with predicted AGN lifetimes which reflects the powerful nature of the current outburst. This is the most powerful central AGN outflow in this small sample. Since the current AGN outburst in Hydra is so powerful, it more than satisfies the heating requirements within the cooling radius. Hence we derive a negative value for the suppression factor.

A2597: It appears that thermal conduction on its own cannot provide sufficient heating except between roughly 4-10 kpc. Without thermal conduction, the required AGN duty cycle is also compatible with predicted AGN lifetimes. A2597 has the largest heating requirements in this sample, followed by A478. Both require more than two orders of magnitude more heating power within the cooling radius than Virgo. It is interesting to note that even a combination of the current AGN heating rate and full Spitzer thermal conduction provide roughly only one fiftieth of the required heating rate within the cooling radius. It therefore seems as if the only means by which a cooling catastrophe can be averted in this system is by an extremely powerful AGN outburst, or a cluster-scale merger.

A1795: On its own, thermal conduction is sufficient to match the heating requirements throughout most of the cluster, although not near 5 kpc. The required AGN duty cycle, in the absence of thermal conduction, of roughly  $4.3 \times 10^7$  yrs is also compatible with predicted AGN lifetimes. For a combination of heating by AGN and thermal conduction a

Name	$L_{\text{mech}}/\alpha/(10^{42}\text{ergs}^{-1})$	$\tau/(10^8\text{yr})$	$L_{\text{cond}}/(10^{42}\text{ergs}^{-1})$	$L_{\text{heat}}/(10^{42}\text{ergs}^{-1})$	$f$
Virgo	$0.052^{+0.028}_{-0.032}$	0.078	13.7	10.7	0.72
Perseus	$5.9^{+3.8}_{-1.2}$	0.28	4360	236	0.05
Hydra	$27.1^{+1.5}_{-2.9}$	1.9	112.8	231	-1.8
A2597	$5.6^{+5.2}_{-1.6}$	0.21	71.0	427	4.8
A2199	$1.3^{+1.9}_{-1.2}$	0.14	797	149	0.16
A1795	$12.5^{+16.8}_{-1.3}$	0.43	1280	465	0.2
A478	$1.9^{+1.0}_{-0.3}$	0.026	2720	1169	0.4

**Table 5.** Assumed average mechanical luminosity per bubble in each cluster based on the observations summarized in Birzan et al. (2004) and assuming a duty cycle of  $10^8$  yrs in (column 2), duty cycle of each AGN in units of  $10^8$  yrs evaluated at the cooling radius (column 3), rate at which energy is supplied to the region within the cooling radius by thermal conduction (column 4), the total required heating rate within the cooling radius (column 5) and the suppression factor for combined heating by AGNs and thermal conduction (column 6). All quantities are evaluated at the cooling radius.

suppression factor of roughly 0.2 is required to achieve the necessary heating.

A478: Thermal conduction alone should be sufficient for matching the heating requirements. In addition, the required AGN duty cycle in the absence of thermal conduction is very short compared with predicted AGN lifetimes. The central AGN outburst in this system is the least powerful in our sample.

These results suggest that heating from AGN, with duty cycles of  $10^8$  yrs, alone is unable to maintain a steady-state, but may result in a quasi steady-state if more powerful outbursts are interspersed with the more common lower power outbursts. Alternatively, it may be that a combination of AGN heating and thermal conduction could provide the necessary heating, at least within the cooling radius, in all but one cluster of our sample: A2597. However, although thermal conduction is a possible heating mechanism of the central regions of galaxy clusters it is still not clear whether thermal conduction actually is an efficient heating mechanism in galaxy clusters. For example, from numerical simulations of the Virgo cluster by Pope et al. (2005), taking in to account thermal conduction with different suppression factors, the observed temperature profiles are most consistent with a suppression factor of between 0-0.1. This is at odds with the value of the suppression factor we have derived for most clusters in this sample. In all cases the effectiveness of thermal conduction must be fine-tuned as a function of radius in order to allow a steady-state of the cluster gas.

It is worth noting that galaxy clusters also need to be heated at radii outside the cooling radius if a time-averaged steady-state is to be maintained. Two possible mechanisms for this are sound waves excited by buoyantly rises bubbles and comparatively rare, but very powerful, AGN outbursts.

It may also be possible to predict which clusters are more likely to experience more powerful AGN outbursts in the near future. For example, if a cooling flow has formed, the fractional decrement in gas temperature between the cooling radius and the cluster centre is likely to be larger than in a cluster which has recently been heated by a large

AGN outburst. Then, if the duty cycle that we have calculated based on the current heating rate, required to maintain a steady state, is much less than  $10^8$  yrs, then we may predict that a powerful outburst is imminent.

Based on the above criteria it seems that in our sample A478 and A2597 are the clusters most likely to experience a powerful AGN outburst in the near future. Virgo appears also to be a candidate for an imminent outburst, however, the relatively small temperature difference between the cluster center and the cooling radius indicates that it may recently have experienced sufficient heating.

Our results for the required heating rates indicate that, for our initial estimate of the AGN duty cycles, if buoyant plasma bubbles are the only heating mechanism by which clusters are heated, then, of our small sample, only the AGN at the centre of Hydra is currently injecting sufficient energy to heat the gas within several multiples of the cooling radius. For the remaining six clusters, the energy available in the form of plasma bubbles is only sufficient to provide the required heating within a relatively small fraction (roughly 0.1-0.5) of the cooling radius. This significant energy deficit implies that these clusters may not be in a steady-state, or that the AGNs are active far more frequently at the centres than outside of clusters.

A possible scenario which is consistent with our results is that AGNs in general produce only relatively small or moderately powerful outbursts, such as we observe in the majority of clusters, which delay the occurrence of a cooling catastrophe by a small amount each time. These small heating events may occur too infrequently to prevent the formation of a cooling flow and the temperature gradient grows with time. Eventually sufficient material is accreted by the central galaxy to initiate an extremely energetic outburst such as those seen in Cygnus-A and Hydra-A. This would also allow the heating of material at radii which are hard to reach with lower power outbursts. In this way the moderately powerful AGN outflows observed in most clusters only delay more energetic events. Such a scenario for clusters, small-scale AGN heating interspersed occasionally

with more energetic events, evolution is complex and would have to be modelled numerically.

## 8 ACKNOWLEDGEMENTS

We especially thank David Rafferty and Brian McNamara for the A2597 data which comprises both the latest data and calibrations (Rafferty, D.A, et al. 2005, in preparation), Steve Allen and Ming Sun for the A478 data which also comprises the latest data and calibrations. Also, Larry David for the Hydra data, Jeremy Sanders for the Perseus data, Stefano Ettori for the A1795 data and Timothy Dennis for additional copies of the A2597, A478, A1795 data. ECDP thanks the Southampton Escience Centre for funding in the form of a studentship, GP and CRK thank PPARC for rolling grant support. We also thank the anonymous referee for many useful comments which improved the paper.

## REFERENCES

Allen S. W., Schmidt R. W., Fabian A. C., 2001, *MNRAS*, 328, L37  
 Birzan L., Rafferty D. A., McNamara B. R., Wise M. W., Nulsen P. E. J., 2004, *ApJ*, 607, 800  
 Brüggén M., 2003, *ApJ*, 593, 700  
 Brüggén M., Kaiser C. R., 2002, *Nat.*, 418, 301  
 Burns J. O., 1990, *Bull. Am. Astron. Soc.*, 22, 821  
 Carilli C. L., Taylor G. B., 2002, *ARA&A*, 40, 319  
 Cho J., Lazarian A., Honein A., Knaepen B., Kassinos S., Moin P., 2003, *ApJ*, 589, L77  
 Choudhuri A., 1998, *The Physics of Fluids and Plasmas, an introduction for astrophysicists*. Cambridge University Press  
 Churazov E., Brüggén M., Kaiser C. R., Böhringer H., Forman W., 2001, *ApJ*, 554, 261  
 Churazov E., Forman W., Jones C., Böhringer H., 2003, *ApJ*, 590, 225  
 David L. P., Nulsen P. E. J., McNamara B. R., Forman W., Jones C., Ponman T., Robertson B., Wise M., 2001, *ApJ*, 557, 546  
 Dennis T. J., Chandran B. D. G., 2005, *ApJ*, 622, 205  
 Edge A. C., 2001, *MNRAS*, 328, 762  
 Ettori S., Fabian A. C., Allen S. W., Johnstone R. M., 2002, *MNRAS*, 331, 635  
 Fabian A. C., 1994, *ARA&A*, 32, 277  
 Fabian A. C., Celotti A., Blundell K. M., Kassim N. E., Perley R. A., 2002, *MNRAS*, 331, 369  
 Gaetz T. J., 1989, *ApJ*, 345, 666  
 Ghizzardi S., Molendi S., Pizzolato F., De Grandi S., 2004, *ApJ*, 609, 638  
 Johnstone R. M., Allen S. W., Fabian A. C., Sanders J. S., 2002, *MNRAS*, 336, 299  
 Kaiser C. R., Pavlovski G., Pope E. C. D., Fangohr H., 2005, *MNRAS*, 359, 493  
 McNamara B. R., Wise M. W., Nulsen P. E. J., David L. P., Carilli C. L., Sarazin C. L., O’Dea C. P., Houck J., Donahue M., Baum S., Voit M., O’Connell R. W., Koekemoer A., 2001, *ApJ*, 562, L149  
 Nipoti C., Binney J., 2005, *MNRAS*, pp 535–+

Pope E. C. D., Pavlovski G., Kaiser C. R., Fangohr H., 2005, *MNRAS*, 364, 13  
 Reynolds C. S., McKernan B., Fabian A. C., Stone J. M., Vernaleo J. C., 2005, *MNRAS*, 357, 242  
 Robinson K., Dursi L. J., Ricker P. M., Rosner R., Calder A. C., Zingale M., Truran J. W., Linde T., Caceres A., Fryxell B., Olson K., Riley K., Siegel A., Vladimirova N., 2004, *ApJ*, 601, 621  
 Ruszkowski M., Begelman M. C., 2002, *ApJ*, 581, 223  
 Sanders J. S., Fabian A. C., Allen S. W., Schmidt R. W., 2004, *MNRAS*, 349, 952  
 Spitzer L., 1962, *Physics of Fully Ionized Gases*. Wiley-Interscience, New York  
 Sun M., Jones C., Murray S. S., Allen S. W., Fabian A. C., Edge A. C., 2003, *ApJ*, 587, 619  
 Sutherland R., Dopita M., 1993, *ApJ Supp.*, 88, 253  
 Tabor G., Binney J., 1993, *MNRAS*, 263, 323  
 Voigt L. M., Fabian A. C., 2004, *MNRAS*, 347, 1130  
 Voigt L. M., Schmidt R. W., Fabian A. C., Allen S. W., Johnstone R. M., 2002, *MNRAS*, 335, L7  
 Zakamska N. L., Narayan R., 2003, *ApJ*, 582, 162